Changes in Organization of the Endoplasmic Reticulum during *Xenopus* Oocyte Maturation and Activation⊡

Mark Terasaki,*† Linda L. Runft,* and Arthur R. Hand‡

Departments of *Physiology and ‡Pediatric Dentistry, University of Connecticut Health Center, Farmington, Connecticut 06032

The organization of the endoplasmic reticulum (ER) in the cortex of *Xenopus* oocytes was investigated during maturation and activation using a green fluorescent protein chimera, immunofluorescence, and electron microscopy. Dense clusters of ER developed on the vegetal side (the side opposite the meiotic spindle) during maturation. Small clusters appeared transiently at the time of nuclear envelope breakdown, disappeared at the time of first polar body formation, and then reappeared as larger clusters in mature eggs. The appearance of the large ER clusters was correlated with an increase in releaseability of Ca^{2+} by IP_3. The clusters dispersed during the Ca^{2+} wave at activation. Possible relationships of ER structure and Ca^{2+} regulation are discussed.

INTRODUCTION

In essentially all species that have been examined so far, a central physiological event at fertilization is an intracellular Ca^{2+} wave that begins at the sperm entry site (Stricker, 1999). Two major consequences of the transient increase in cytosolic Ca^{2+} are the modification of the extracellular matrix through cortical granule exocytosis and reinitiation of the cell cycle (Kline, 1988; Jaffe *et al.*, 2000). Ca^{2+} is released from internal membrane stores, very likely the endoplasmic reticulum (ER) (Eisen and Reynolds, 1985; Han and Nuccitelli, 1990). In several species, Ca^{2+} release is mediated by the second messenger IP_3, which opens Ca^{2+} channels in the ER; this has been shown in hamster (Miyazaki *et al.*, 1992), mouse (Miyazaki *et al.*, 1993), frog (Nuccitelli *et al.*, 1993; Stith *et al.*, 1993; Snow *et al.*, 1996; Runft *et al.*, 1999), starfish (Carroll *et al.*, 1997), and sea urchins (Carroll *et al.*, 1999; Shearer *et al.*, 1999).

Maturation is the process by which oocytes become competent to be fertilized. Immature oocytes of most species are arrested at prophase of meiosis I. At a time appropriate to the reproductive cycle of the species, oocyte maturation is initiated, usually by a hormone. Attempts to fertilize oocytes before the completion of maturation lead to abnormal development; the male and female DNA do not pair correctly, and egg activation does not occur properly. This has to led to the concept of two parallel, interdependent processes during maturation (Masui and Clarke, 1979): resumption of the meiotic reduction divisions necessary for the combination of maternal and paternal genomes, and "physiological" or "cytoplasmic" maturation, involing changes that are necessary for the egg to activate normally after insemination.

There are several indications that fundamental changes occur in Ca^{2+} physiology during maturation. From quantitative injections of IP_3, it was found that 100-fold less IP_3 was sufficient to release the same amount of Ca^{2+} in mature starfish eggs than in immature oocytes (Chiba *et al.*, 1990). A similar change has been seen during hamster (Fujiwara *et al.*, 1993) and mouse oocyte maturation (Mehlmann and Kline, 1994). Among the other indications of a change in Ca^{2+} physiology are a smaller Ca^{2+} transient in inseminated immature starfish oocytes (Chiba *et al.*, 1990; Stricker *et al.*, 1994), a change in Na^+–Ca^{2+} exchange in mouse oocytes (Carroll, 2000), and a twofold increase in IP_3 receptors in mouse oocytes during maturation (Mehlmann *et al.*, 1996).

The ER, which is very likely the source of Ca^{2+} at fertilization, also changes during maturation. There are structural ER changes in oocytes in all six species examined to date: frog (Campanella and Andreucetti, 1977; Gardiner and Gray, 1983; Campanella *et al.*, 1984; Charbonneau and Gray, 1984), sea urchin (Henson *et al.*, 1990), starfish (Jaffe and Terasaki, 1994), mouse (Mehlmann *et al.*, 1995), hamster (Shiraishi *et al.*, 1995), and the nemertean worm *Cerebratulus lacteus* (Stricker *et al.*, 1998). The ER also undergoes drastic structural changes at fertilization in some species but not others (see DISCUSSION). The present study describes changes in the ER organization during maturation and activation in *Xenopus*, where as noted above, Ca^{2+} release from the ER has been shown to be caused by the production of

---

⊡ Online version of this article contains video material for Figures 9 and 10. Online version available at www.molbiocell.org.

† Corresponding author. E-mail address: terasaki@neuron.uchc.edu.

IP$_3$. We found changes in ER organization that parallel changes in Ca^{2+} release properties during maturation, as well as changes in ER organization when it releases Ca^{2+} at activation.

MATERIALS AND METHODS

Xenopus Oocytes

Wild-type or albino female *Xenopus laevis* frogs were purchased from Nasco (Fort Atkinson, WI). Methods for obtaining oocytes were similar to those described previously by Gallo *et al.* (1995). Briefly, pieces of ovary were incubated in collagenase (2%; Sigma, St. Louis, MO) and shaken continuously at 100 rpm at room temperature for 1 hr 45 min. The oocytes were washed in 100 mM K phosphate, pH 6.5, and 0.1% BSA, then sorted using a dissecting scope (Duesbery and Masui, 1993), and maintained in OR3 buffer (50% Leibovitz's L-15 medium, 15 mM HEPES, pH 7.8, 100 μg/ml gentamicin).

Oocytes were matured in vitro by incubation at 18°C in 1 μg/ml progesterone (Steraloids, Inc., Newport, RI) (stock was dissolved at 10 mg/ml in ethanol and used for no longer than 1–2 wk). Germinal vesicle breakdown (GVBD) was noted by the appearance of a white spot in the pigment of wild-type oocytes and by the condensation of a dark spot on albino oocytes (Runft *et al.*, 1999). Eggs were considered to be fully mature (arrested at metaphase II) at 3 h after GVBD (Gallo *et al.*, 1995). In this article, the term "oocyte" will be used to refer to immature oocytes, and "egg" will be used interchangeably with "mature oocyte." Modified Ringer's solution (100 mM NaCl, 1.8 mM KCl, 1 mM MgCl$_2$, 2 mM CaCl$_2$, 5 mM HEPES, pH 7.8) was used.

Microinjection

Injections were done using a Picospritzer (General Valve Corporation, Fairfield, NJ) with the air pressure set at 30 psi and a pulse duration of 40–200 ms. Solutions to be injected were backfilled into microfilament glass micropipettes that had tips broken to a diameter of ~18 μm (Runft *et al.*, 1999).

mRNA coding for the green fluorescent (GFP)–KDEL construct (Terasaki *et al.*, 1996) was made using mMessage mMachine kit (Ambion, Austin, TX). It was dissolved in water and injected to a final concentration in the oocyte of ~20 μg/ml. Rhodamine dextran (3 kDa) (Molecular Probes, Eugene, OR) was dissolved at 10 mg/ml in injection buffer (100 mM potassium glutamate, 10 mM HEPES, pH 7.0).

Microscopy

Oocytes or eggs were mounted in a simple silicone rubber chamber for microscopic observations. The silicone rubber (calendared sheet; North American Reiss, Blackstone, VA) was 0.03 inches (0.76 mm) thick with a ~3 × 3 mm square hole cut out with a razor blade. A coverslip was used for the top and bottom of the chamber so that both animal and vegetal halves could be observed.

A MRC600 confocal microscope (Bio-Rad, Cambridge, MA) with a krypton argon laser was coupled to an upright microscope (Axioskop, Carl Zeiss, Thornwood, NY). A 63× plan-apo numerical aperture 1.4 objective lens was used for imaging.

Electron Microscopy Methods

Oocytes or eggs were fixed in 2.5% glutaraldehyde in 0.1 M sodium cacodylate buffer, pH 7.4, for 2–3 h, rinsed in 0.1 M cacodylate buffer, then post-fixed for 1 h with 1% OsO$_4$ and 0.8% potassium ferricyanide in cacodylate buffer. They were rinsed thoroughly in distilled water and stained in 0.5% aqueous uranyl acetate for 1 h. They were dehydrated in ethanol and embedded in Poly/Bed resin (Polysciences, Warrington, PA). Ultrathin sections were stained with uranyl acetate and lead citrate and examined in a transmission electron microscope (CM-10, Philips, Eindhoven, The Netherlands).

Immunofluorescence Methods

Oocytes or eggs were fixed in methanol with 1% formaldehyde (Yumura and Fukui, 1985). The fixative was made by adding 0.33 ml formalin to 10 ml methanol in a scintillation vial and was stored in a −80°C freezer. Oocytes were fixed by dropping the eggs into the fixative and returning the vial to the freezer. After 1.5 h, the vial was allowed to warm up at room temperature for 30 min. The oocytes were then rehydrated in 2:1 methanol:PBS for >20 min, 1:2 methanol:PBS for >20 min, then PBS. Using a dissecting microscope, the vitelline envelope was removed by scoring the vitelline envelope on the animal half with several passes with a microinjection needle, followed by peeling off the vitelline envelope with fine forceps.

For immunofluorescence labeling, fixed oocytes or eggs were incubated in primary antibody for 1–1.5 h, washed several times over a period of 10–20 min, then incubated in second antibody for 1 h, followed by another wash and mounting in a silicone rubber observation chamber.

For IP$_3$ receptor immunofluorescence, an affinity-purified rabbit polyclonal antibody to the C-terminal 19 amino acids of the rat type 1 IP$_3$ receptor was used (Research Genetics, Huntsville, AL) (Runft *et al.*, 1999). A 1:200 dilution of the antibody (2.5 mg/ml) was used for immunofluorescence, with a 1:50 dilution of second antibody (rhodamine goat anti-rabbit IgG; ICN, Costa Mesa, CA). For nuclear pores of annulate lamellae, mAb 414 (Berkeley Antibody Company, Richmond, CA) was used. A 1:100 dilution of the 1 mg/ml antibody was used, with a 1:50 dilution of second antibody (rhodamine goat anti-mouse IgG).

Caged IP$_3$ Experiments

Albino oocytes were coinjected with Ca^{2+} green 10-kDa dextran (Molecular Probes) and caged IP$_3$ (D-*myo*-inositol 1,4,5-trisphosphate, P$^{4(5)}$-1-(2-nitrophenyl) ethyl ester; Calbiochem, La Jolla, CA). All injections were 50 nl (5% of the total oocyte volume), and IP$_3$ concentrations given in the text refer to the final concentrations in the oocyte cytoplasm. Some oocytes injected with caged IP$_3$ were matured in vitro by incubation in progesterone. To uncage the IP$_3$, oocytes at various stages of maturation were placed in 500 μl of one-third diluted modified Ringer's solution and exposed to UV light from a 100-W mercury arc lamp that was passed through a 330-nm bandpass filter (Omega Optical, Brattleboro, VT). The UV light was focused on the oocyte or egg through a 5×, 0.15 N.A. Plan Neofluar objective. Changes in Ca^{2+} green dextran fluorescence were detected using a 5×, 0.15 N.A. Plan Neofluar objective and a photomultiplier tube connected through a current-to-voltage converter to a chart recorder (described in Chiba *et al.*, 1990). Use of a slider to quickly change fluorescence filters allowed for rapid alternation between blue and UV light. Albino oocytes were used, because the pigment present in wild-type oocytes absorbs the light used to measure changes in Ca^{2+} levels.

Extracellular Dextran

Rhodamine dextran (3 kDa) was dissolved at 0.3–0.6 mg/ml in 1× modified Ringer's solution. Eggs were transferred to a pool of this solution on parafilm, then put into a silicone rubber chamber with an open side to allow access for prick activation with a microneedle; the egg was maneuvered so that the vegetal side faced the objective, and a coverslip was lowered onto the chamber. The eggs were prick-activated on the stage of the microscope with a 10× objective lens, then the lens was switched to the 63× oil immersion lens and focused on the egg surface next to the coverslip. The confocal microscope was set to scan continuously; images were recorded on an optical memory disk recorder (TQ-3038F; Panasonic, Secaucus, NJ) that was triggered with a special circuit to record each scan (http://terasaki.uchc.edu/trigger.html). The data were digitized to a Macintosh computer via firewire using a Sony DVMC-DA1 converter.

RESULTS

ER Organization in Immature Oocytes versus Mature Eggs

Ovulated frog eggs are arrested at second meiotic metaphase. Maturation can be conveniently studied in vitro using isolated immature oocytes, which are arrested at prophase of meiosis I; after application of the hormone progesterone, GVBD occurs at ~8–12 h, and the meiotic cell cycle progresses to the meiosis II metaphase arrest ~3 h after GVBD. At this time, the "mature" eggs are fertilizable, that is, they have acquired the ability to undergo normal development after addition of sperm. The polar bodies are extruded in the center of the dark, pigmented "animal" half of the frog egg; this site is called the "animal pole," whereas the unpigmented half is called the "vegetal" half.

GFP was previously targeted to the lumen of the ER by using the construct GFP–KDEL in starfish (Terasaki *et al.*, 1996) and sea urchins (Terasaki, 2000). This construct consists of the S65T mutant of GFP, a signal sequence from sea urchin ECast/PDI (Lucero *et al.*, 1994), and a KDEL retention sequence at the C terminal. mRNA coding for GFP–KDEL was injected into *Xenopus* immature oocytes, and the fluorescence that developed overnight was observed by confocal microscopy. Because of scattering or absorption by the large yolk platelets, it is difficult to obtain images very deep in the interior. Another obstacle is the dense distribution of pigment granules on the animal half. Observations were confined to the first ~10 μm from the surface.

A relatively uniform three-dimensional network was seen in the cortex of both animal and vegetal sides of immature oocytes (Figure 1). The network appears to consist of tubules and individual cisternae (i.e., not stacked cisternae). In the vegetal half, ~5 μm from the surface, there were long, narrow, dense islands, ~4 μm in width by 20–30 μm in length (Figure 2A). Their approximate density was 1–3/100 μm^2 (i.e., 10 × 10-μm-square patch). They corresponded in size, shape, and distribution to immunofluorescence labeling with a nuclear pore antibody (mAb 410) (Figure 2B). This shows that the GFP–KDEL-labeled islands are annulate lamellae, which are stacks of cisternae with surface membranes that are densely packed with nuclear pores (Kessel, 1992). Annulate lamellae of expected size and location were seen in thin-section electron micrographs of the vegetal half (Figure 2C). These observations are consistent with a previous electron microscopic study of whole sections of oocytes, which found a large abundance of annulate lamellae in the vegetal cortex (Imoh *et al.*, 1983), and with freeze-fracture electron microscopy (Larabell and Chandler, 1988).

In mature eggs, the ER in the animal side appeared unchanged, but the ER on the vegetal side had undergone a striking reorganization. The annulate lamellae had disappeared. Clusters of dense ER of irregular size and shape were present in the cortex (Figure 3); they were present throughout the unpigmented region of the egg up to the boundary of the pigmented region. The larger clusters had dimensions of ~3–5 μm. We counted only those clusters >1 μm in size; these were present at a density of ~1.0–1.5/100 μm^2. There is some variation in eggs from different animals. In Z-section image sequences, the clusters were seen to be three-dimensional, with a thickness of ~4 μm (Figure 3). Usually, the clusters appeared to be located directly adjacent
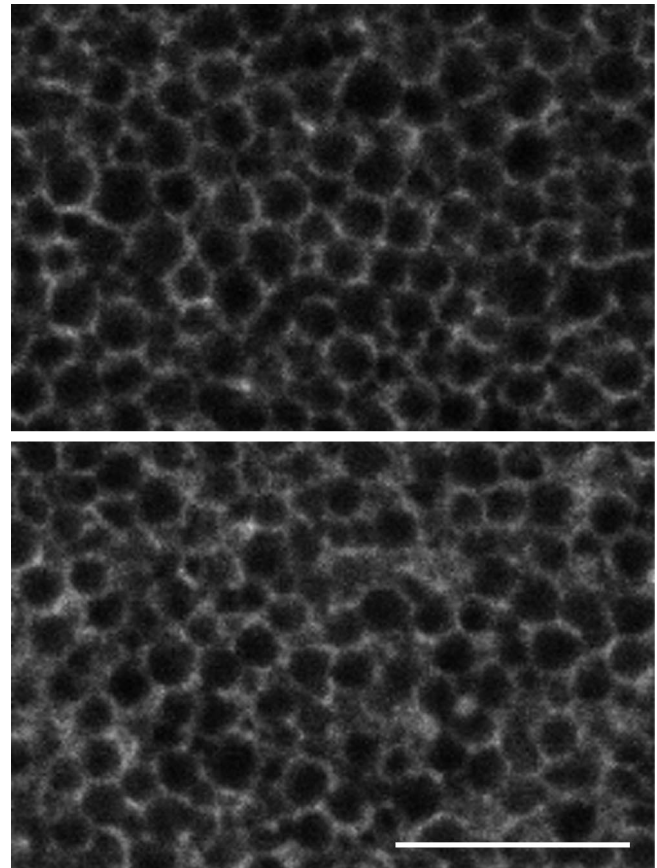
Figure 1. High-magnification view of GFP–KDEL labeling in the cortex of immature oocytes. The top panel shows labeling in the animal half, and the bottom panel shows labeling in the vegetal half. On both sides, the ER has a network appearance, probably consisting of tubules and/or single (unstacked) cisternae. The pattern on the vegetal side has a small amount of patches. Cortical granules and other organelles are present in the dark spaces between the ER. Bar, 10 μm.

to the surface, but occasionally there were eggs in which the clusters were located 1–2 μm from the surface. The clusters were distributed throughout the unpigmented vegetal cortex up to the boundary with the pigmented cortex. Time lapse sequences of GFP–KDEL-labeled ER in living eggs showed that the clusters were stable over a period of at least 10 min. Small clusters sometimes changed shapes, and the edges of most clusters seemed to be moving. The tubular networks between the clusters showed the most motility.

In high-resolution images, details could not be resolved in the interior of the clusters, suggesting either the presence of a large swollen cistern of ER or that the ER membranes are so tightly packed in the clusters that they cannot be resolved by light microscopy. To address this, the ER distribution was imaged in relation to 3-kDa rhodamine dextran injected into the cytoplasm. This marker diffuses throughout the cytosol and shows large organelles such as yolk platelets or cortical granules in negative image. Comparison of the 3-kDa rhodamine dextran and GFP–KDEL images showed that the ER network extends between most of the large organelles in the
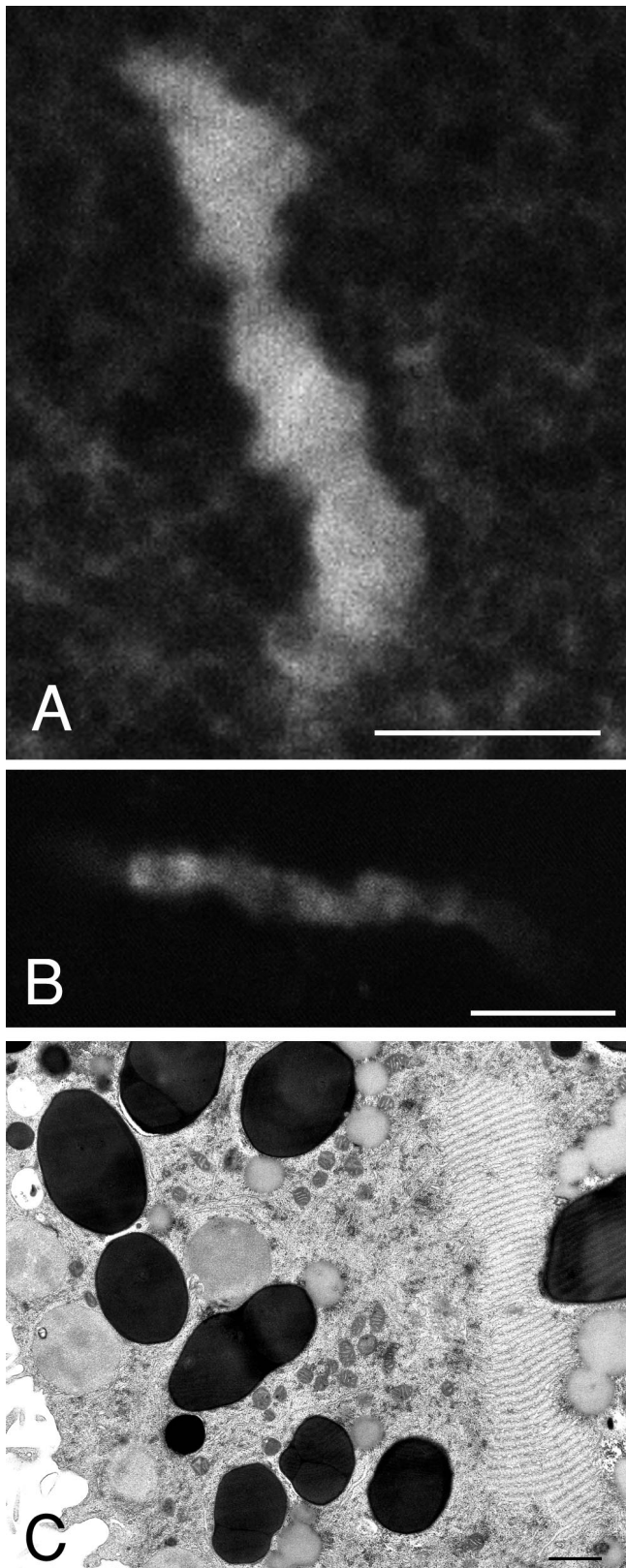
cortex (Figure 4). The GFP–KDEL-labeled clusters and 3-kDa dextran corresponded well in the double-label images. This showed that cytosolic molecules can diffuse into the cluster regions and is evidence that a cluster is not a walled-off region of cytoplasm, as occurs with a multivesicular body, nor is it a large swollen cisterna of ER.

Thin-section electron micrographs of mature eggs showed structures that corresponded well in size and distribution to the GFP–KDEL-labeled clusters (Figure 5). In high-magnification electron micrographs, the clusters appeared to be packed elements of smooth ER of a complex geometry. The electron-dense particles interspersed in the clusters had the characteristic appearance and distribution of glycogen granules.

IP_3 causes release of Ca^{2+} from the ER at fertilization (Nuccitelli *et al.*, 1993; Runft *et al.*, 1999), so we examined the IP_3 receptor distribution by immunofluorescence with an antibody to the type 1 IP_3 receptor. This antibody was shown previously to recognize one major band on a blot of *Xenopus* eggs (Runft *et al.*, 1999). Immunofluorescence showed dense accumulations of IP_3 receptors with a size and distribution very similar to that of the GFP–KDEL-labeled clusters (Figure 6). There were no accumulations of IP_3 receptors in the animal half at the surface, but only a staining pattern that seemed to correspond to a network staining. In addition, the antibody stained only the network in immature oocytes.

ER Cluster Formation Is Related to Cell Cycle

The development of the ER clusters on the vegetal side was observed during maturation. Clusters first appeared at about the time of white spot formation/germinal vesicle breakdown. These clusters were smaller and less distinct than those present in mature eggs. The clusters disappeared and then reappeared by the time of second meiotic metaphase arrest. The time sequence of cluster appearance and disappearance was imaged in individual eggs (Figure 7). The small clusters were present for 1–2 h and then absent for ~1 h, and then they reappeared as large clusters (Figure 7B). The timing suggests that small clusters appear during meiosis I metaphase and disappear during first polar body formation, perhaps at anaphase, and then large clusters appear during meiosis II metaphase.

IP_3 Sensitivity during Maturation

Starfish, hamster, and mouse oocytes have been shown to be more sensitive to IP_3-induced Ca^{2+} release after undergoing maturation (Chiba *et al.*, 1990; Fujiwara *et al.*, 1993; Mehlmann and Kline, 1994). This suggests that these oocytes

Figure 2. Annulate lamellae in the vegetal half of immature oocytes. (A) An example of a long, dense island of GFP–KDEL labeling. These are present ~5 μm in from the surface. Bar, 10 μm. (B) Immunofluorescence labeling with mAb 414 antibody to nuclear pores showing a similar structure as seen with GFP–KDEL labeling. Bar, 10 μm. (C) Thin-section electron micrograph in the vegetal cortex showing a long, narrow structure on the right side with the characteristic appearance of an annulate lamellae. The long, dense islands labeled by GFP–KDEL therefore correspond to annulate lamellae. Bar, 1 μm.
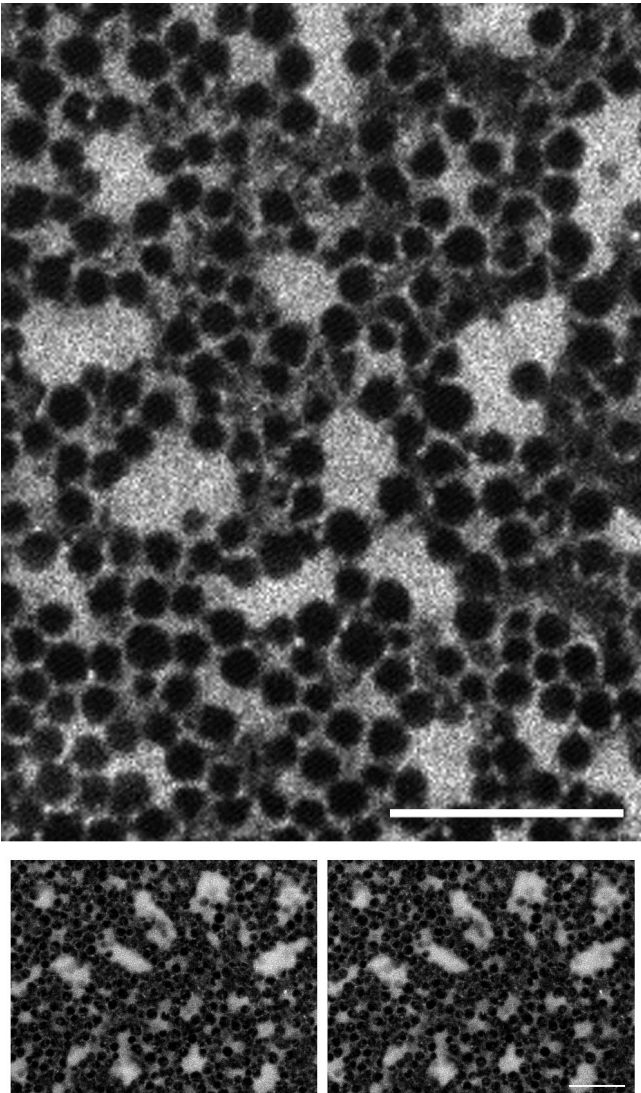
Figure 3. High-magnification view of GFP–KDEL labeling in the vegetal cortex of mature oocytes. Clusters of dense GFP–KDEL labeling have appeared during maturation. Bottom panels, stereo pair showing that the clusters extend into the cytoplasm. Bar, 10 μm.

Figure 4. Double labeling of GFP–KDEL (top panel) and cytosolic 3-kDa rhodamine dextran (bottom panel) in the vegetal cortex of mature oocytes. The cytosolic dextran penetrates into the cluster regions labeled by the GFP–KDEL. This indicates that the cluster is not a single swollen ER cisternae. This conclusion is consistent with the electron micrographs of ER clusters in Figure 5. The cortical granules and other large organelles in the cortex are seen in negative image in the dextran image, and the ER network outside the clusters is seen to run between these organelles. Bar, 10 μm.

undergo changes in Ca^{2+} regulation in preparation for fertilization. We tested whether there is a similar change in IP_3 sensitivity in frog oocytes and whether there is a correlation with the changes in the ER.

We first compared IP_3-induced Ca^{2+} release in immature oocytes versus mature eggs. Immature albino oocytes were coinjected with Ca^{2+} green dextran and caged IP_3 at three different concentrations (0.1, 1, and 10 μM), and then half of these oocytes were matured by the addition of progesterone. Immature oocytes and matured eggs (at 3–4 h after GVBD) were exposed to UV light to uncage the IP_3. Ca^{2+} levels were monitored by Ca^{2+} green dextran fluorescence. At all three concentrations of caged IP_3, mature eggs released significantly more Ca^{2+} compared with immature oocytes (Table 1

and Figure 8); however, mature eggs released similar amounts of Ca^{2+} at all three IP_3 concentrations, whereas oocytes released significantly more Ca^{2+} as the concentration of IP_3 was increased (Table 1). This indicates that both eggs and oocytes contain IP_3-responsive Ca^{2+} stores, but the Ca^{2+}-releasing machinery in mature eggs is more sensitive to IP_3 than it is in oocytes.

To determine when this increase in IP_3 sensitivity occurs, we then monitored IP_3-induced Ca^{2+} release during maturation. Immature oocytes were coinjected with Ca^{2+} green dextran and 1 μM caged IP_3, and their ability to release Ca^{2+} was monitored at each hour after progesterone addition. Ca^{2+} release in the maturing oocytes did not change significantly during the period from progesterone addition up to GVBD. Because structural changes occur in the ER at GVBD and at ~1 h after GVBD (Figure 7), the ability of maturing oocytes to release Ca^{2+} at GVBD and at every hour after
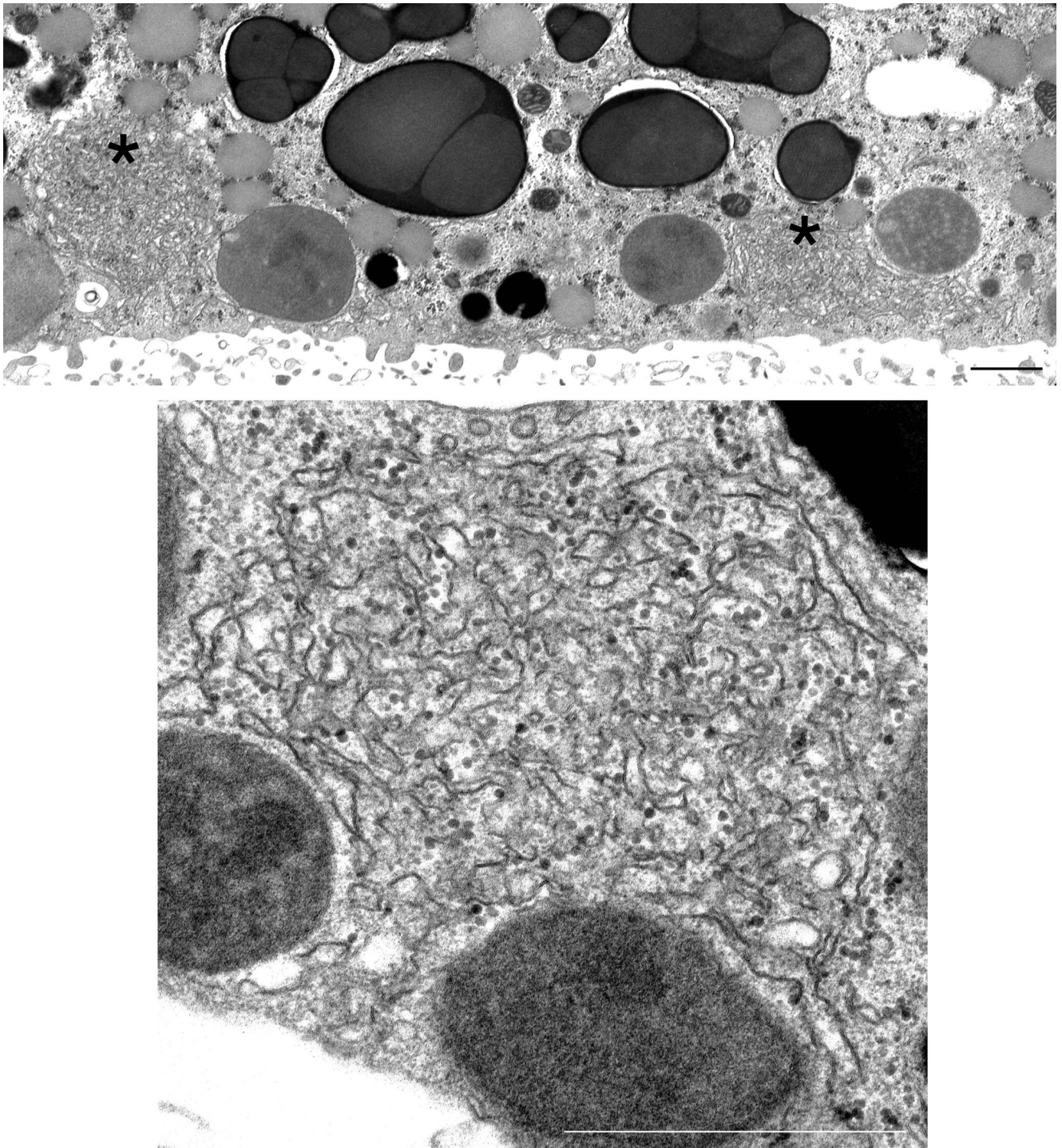
Figure 5. Thin-section electron micrographs of ER clusters in the vegetal cortex of a mature oocyte. The top panel shows a low magnification view with two clusters that are denoted by black asterisks. The bottom panel is a high-magnification view of a cluster. The cluster consists of smooth-surfaced tubules and/or cisternae in a complicated three-dimensional arrangement. Bars, 10 μm.

GVBD was examined. IP$_3$ sensitivity of Ca^{2+} release was not significantly different when oocytes were compared at GVBD, 1 h after GVBD, and 2 h after GVBD (Table 2). Only

at 3 h after GVBD did the ability of eggs to release Ca^{2+} in response to activating 1 μM caged IP$_3$ increase significantly compared with that in immature oocytes (Table 2). These
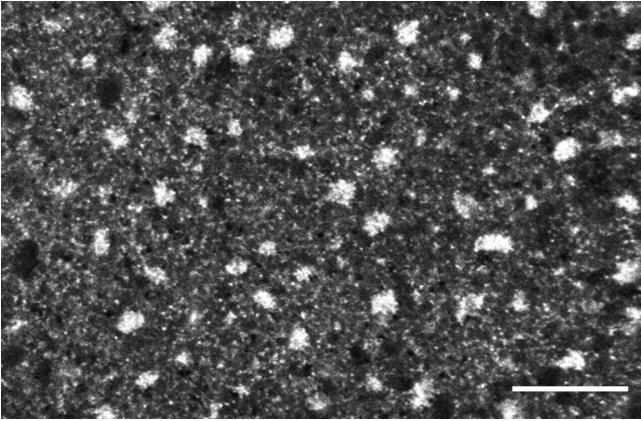
Figure 6. Immunofluorescence with antibody to IP$_3$ receptor in the vegetal half of a mature oocyte. The labeling shows a similarity to GFP–KDEL labeling of clusters. This indicates that IP$_3$ receptors are present in the clusters and that the clusters are likely to be sites of Ca^{2+} release at fertilization. Bar, 10 μm.

results indicate that the Ca^{2+}-releasing machinery becomes more sensitive to IP$_3$ ~3 h after GVBD. This is also about the time that the oocytes enter metaphase II and become mature eggs (Gard, 1992) and when the large ER clusters appear.

ER Clusters Disperse during Activation or Fertilization

Mature eggs expressing GFP–KDEL were artificially activated by pricking the egg surface with a micro-needle. The clusters became altered in a wave 1–3 min after pricking (Figure 9; see movie act.mov at www.molbiocell.org or at http://room2.mbl.edu/xeno/act.mov). The timing corresponded approximately to the time required for the Ca^{2+} wave to reach the imaged area from the site of pricking. The clusters became dispersed and did not reappear after activation; in particular, they were not present during the cortical rotation that begins ~45 min after activation (Houliston and Terasaki, unpublished observations). We previously used photobleaching techniques to show that the ER becomes transiently discontinuous at fertilization in starfish eggs (Terasaki *et al.*, 1996). Unfortunately, *Xenopus* eggs appeared to be very sensitive to the high-intensity laser light required for photobleaching GFP; the cytoplasm in the region of the bleach contracted, and there was no recovery of fluorescence, even in unactivated eggs where the ER is expected to be continuous, so we were unable to use this technique to assess the continuity of the ER.

Experiments were performed to determine the temporal relationship between Ca^{2+} release from the ER and the changes in ER structure. It was not possible to image cytosolic Ca^{2+} and ER structure simultaneously, because of the lack of a longer-wavelength bright fluorescent Ca^{2+} indicator. The relationship of Ca^{2+} and ER structure was examined indirectly by imaging each with respect to surface changes. It was shown previously that extracellular markers of fluid space label large spots at the sea urchin egg cortex during fertilization (Terasaki, 1995). The appearance of the spots corresponded exactly with exocytosis of cortical granules as

seen by transmitted light microscopy. The spots correspond to long-lived exocytotic depressions seen in the surface by freeze-fracture microscopy (Chandler and Heuser, 1979). Some of these spots become endosomes in sea urchin eggs (Whalley *et al.*, 1995). We found that similar fluorescent spots appear in a wave-like pattern in activated *Xenopus* eggs. One difference is that the spots seem to shrivel after a few seconds, whereas they do not seem to change in sea urchin. We were unable to show definitively that they correspond with exocytosis because of the difficulty in imaging cortical granules by transmitted light microscopy. For these experiments, we used the appearance of spots to time the ER change with respect to the Ca^{2+} wave.

Extracellular rhodamine dextran was first imaged simultaneously with calcium green dextran. The boundary of the advancing Ca^{2+} wave is very sharp (Runft *et al.*, 1999). The Ca^{2+} wave clearly preceded the appearance of any of the rhodamine dextran labeling in any given region by ~5–7 s (Figure 10; see movies cadx.mov and caer.mov at www.molbiocell.org or at http://room2.mbl.edu/xeno/), after which spots continued to appear in the same region for many seconds. Extracellular rhodamine dextran was then imaged simultaneously with GFP–KDEL. Dispersal of the clusters was gradual, but it appeared that it began after the dextran-labeled spots first appeared. Thus we conclude that the release of Ca^{2+} precedes or coincides with the beginning of the change in ER structure.

DISCUSSION

Several techniques have been used in the past to investigate the organization of the ER in frog oocytes and eggs. Thin-section electron microscopy showed an increased association of ER with cortical granules in mature eggs (Campanella and Andreucetti, 1977; Campanella *et al.*, 1984) and also showed evidence for junctions of ER with plasma membrane that seemed to develop in parallel with the ability to artificially activate eggs (Gardiner and Gray, 1983; Charbonneau and Gray, 1984). Kume *et al.* (1993, 1997) and Parys *et al.* (1994) examined cryosections of fixed oocytes and eggs and showed by immunofluorescence that there is an extensive network of ER in the interior that contains IP$_3$ receptors, particularly near the nucleus. Cortical ER and annulate lamellae have also been observed by freeze-fracture electron microscopy (Larabell and Chandler, 1988). The fluorescent dicarbocyanine dye DiI has been used, but this method is not well suited for the large frog eggs. The dye takes a long time to diffuse throughout the large egg and in the meantime transfers to other compartments by membrane traffic, so it was necessary to look at transient labeling in the neighborhood of a small oil drop (Kume *et al.*, 1997).

We previously used a GFP chimera, GFP–KDEL, to label the ER in starfish and sea urchin eggs (Terasaki *et al.*, 1996; Terasaki, 2000). GFP–KDEL is expected to exist in the ER lumen as a soluble protein. It should serve as a good marker for the ER, although it should be pointed out that it has not yet been demonstrated that soluble lumenal proteins will diffuse throughout all of the ER. A significant advantage of this marker is that it can be observed in living cells, without the limitations of DiI in frog eggs. This eliminates the need for fixation and permeabilization, which are particularly disruptive in the large frog eggs. Another difference in this
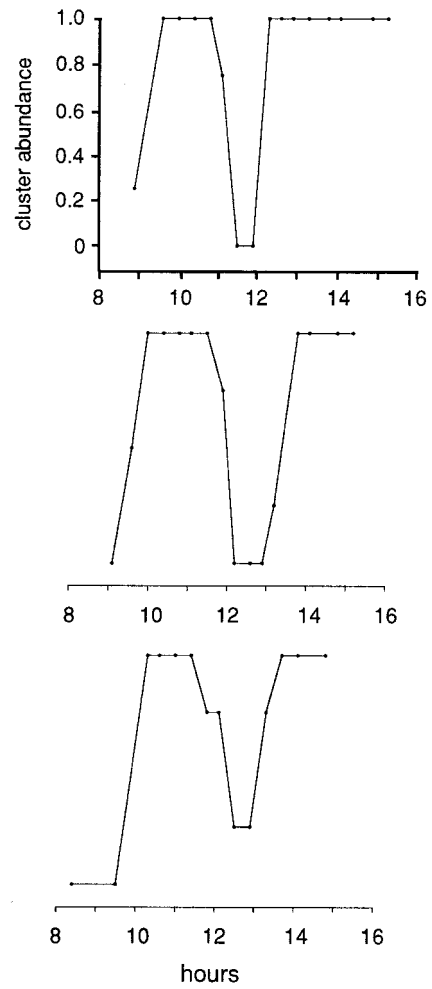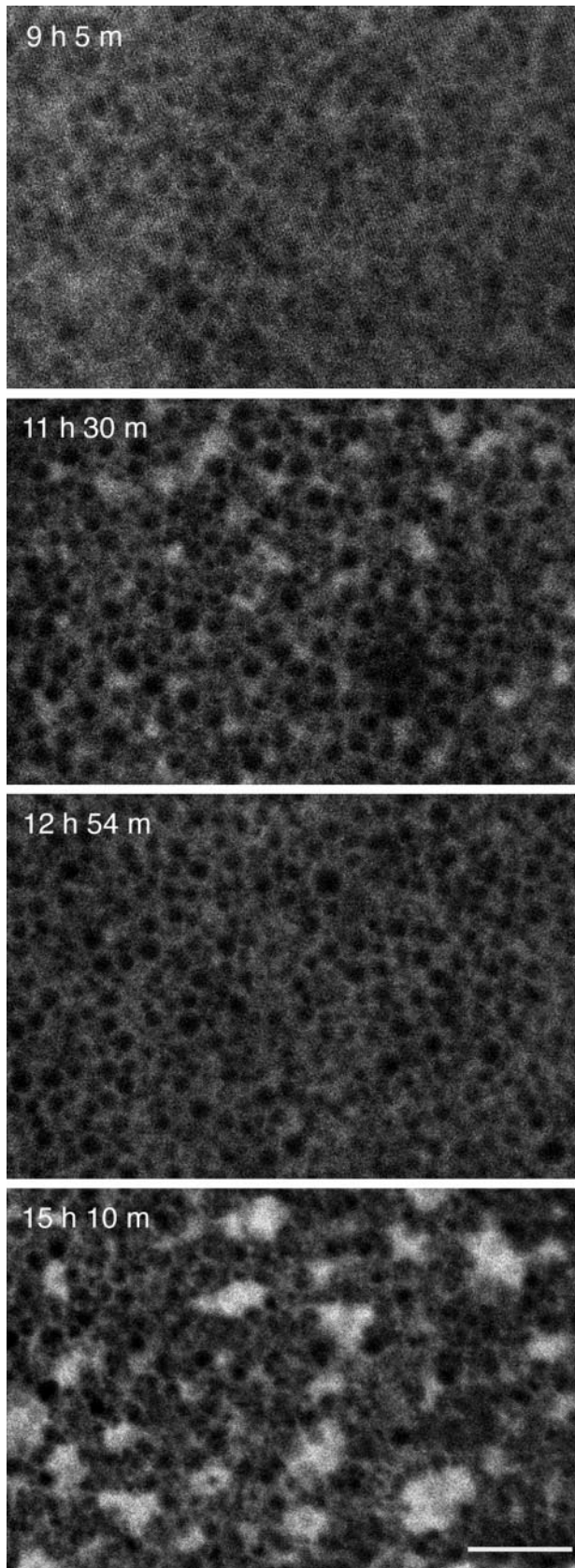
Figure 7. Time course of the appearance of the GFP–KDEL-labeled clusters in the vegetal cortex during maturation. In this experiment, several oocytes were kept in individual dishes; at the various time points, individual oocytes were transferred to the microscope stage for imaging. The images shown were from the same oocyte. The time after addition of progesterone is indicated on the panels. The appearance of the white spot, caused by GVBD, was clearly seen in this oocyte first at 11 h. The image sequence shows the appearance of small clusters at around the time of GVBD, their disappearance at an intermediate time, and then the appearance of large clusters after the egg has become mature. Bar, 10 μm. Each graph shows the time course of the abundance of clusters for three different oocytes during maturation. Cluster abundance was scored visually on a scale between no clusters (0) and maximum number of clusters (1.0). The *x*-axis shows time after addition of progesterone. The graphs for the different oocytes were positioned so that the decrease in clusters is lined up. The middle panel corresponds to the image sequence.

Table 1. Ca^{2+} release in response to IP_3 in oocytes and eggs[a]

Concentration of caged IP_3 injected[b]	Fluorescence after UV exposure[c]	
	Oocytes	Eggs
0.1 μM	0.08 ± 0.04* (10)	0.9 ± 0.07 (10)
1 μM	0.35 ± 0.1* (6)	0.9 ± 0.15 (5)
10 μM	0.6 ± 0.07* (6)	0.8 ± 0.1 (6)

[a] Data are expressed as the mean ± S.D. n = number of eggs tested.

[b] Stage VI oocytes were coinjected with 20-μM Ca^{2+} green dextran and caged IP_3 (concentrations given refer to the final concentration in the cytoplasm). Stage VI oocytes and mature eggs were exposed to UV light for 15 s to uncage the IP_3, and Ca^{2+} green fluorescence was monitored as in Figure 8.

[c] Data for Ca^{2+} green fluorescence in response to IP_3 are expressed as the area under the curve of photomultiplier current as a function of time for a 5-min period after the UV exposure; these values were normalized by dividing by (baseline current × 5 min). Data are presented this way rather than as peak amplitudes, because the peak sometimes occurred during the UV exposure.

* These values are significantly different from the values obtained in mature eggs (unpaired t test, $p < 0.02$).

Table 2. Ca^{2+} release in response to IP_3 at different stages of maturation[a]

Developmental stage[b]	Fluorescence after UV exposure[c]
Stage VI oocyte	0.4 ± 0.2 (6)
At GVBD	0.4 ± 0.2 (6)
1 h after GVBD	0.45 ± 0.2 (6)
2 h after GVBD	0.5 ± 0.2 (6)
3 h after GVBD (mature egg)	0.7 ± 0.2* (6)

[a] Data are expressed as the mean ± S.D. n = number of eggs tested.

[b] Stage VI oocytes were coinjected with 20-μM Ca^{2+} green dextran and 1-μM caged IP_3. Stage VI oocytes and oocytes collected at various time points after progesterone addition were exposed to 5- or 10-s UV light to uncage the IP_3 and Ca^{2+} green fluorescence was monitored as in Figure 8. In each experimental run, the amount of UV used to uncage the IP_3 was determined by finding the shortest time of UV exposure that could induce Ca^{2+} release in mature eggs (in each experimental run, oocytes and eggs were exposed to UV for the same amount of time).

[c] Data for Ca^{2+} green fluorescence in response to IP_3 are expressed as the area under the curve of photomultiplier current as a function of time for a 6-min period after the UV exposure; these values were normalized by dividing by (baseline current × 6 min). Data are presented this way rather than as peak amplitudes, because the peak sometimes occurred during the UV exposure.

* This value is significantly different from the control value obtained from stage VI oocytes (unpaired t test, $p < 0.02$).

study is that the egg cortex was viewed by confocal microscopy en face; this different view has probably also helped us to observe new features of ER organization.
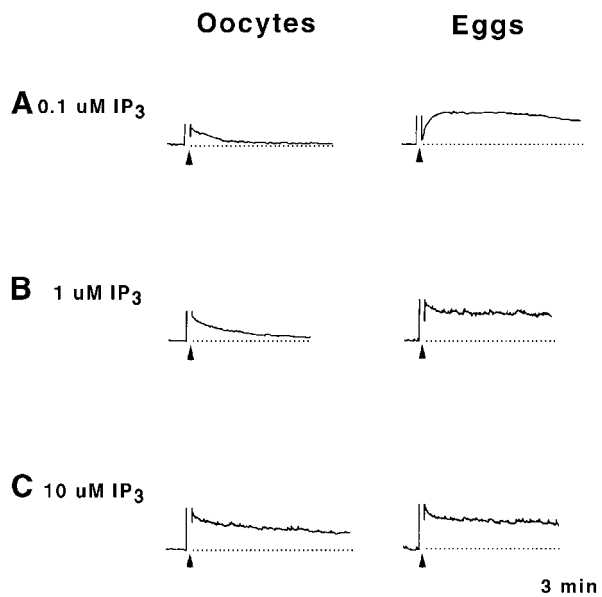
Figure 8. Oocytes are less sensitive to IP_3 than mature eggs. Stage VI oocytes were coinjected with 20 μM Ca^{2+} green dextran and the indicated concentration of caged IP_3. Some of these oocytes were matured in progesterone. During the 15-s period indicated by the arrowhead, the immature oocyte or mature egg (3 h after GVBD) was exposed to UV light to activate the caged IP_3. Traces show Ca^{2+} green fluorescence as a function of time for caged IP_3 at 0.1, 1.0, and 10 μM. The dotted line represents an extension of the baseline. Quantitation of these experiments is shown in Table 1.

GFP–KDEL-expressing mature eggs showed the presence of clusters of ER in the vegetal cortex. Rhodamine dextran in the cytosol penetrates the cluster regions labeled by GFP–KDEL, showing that the clusters are composed of densely packed ER membranes rather than a large dilated ER cisterna. Electron micrographs of the ER clusters are consistent with this conclusion also. Kume *et al.* (1993) showed a distinct IP_3 receptor immunofluoresence labeling in the vegetal cortex of mature eggs that is dispersed in fertilized eggs, some of which could correspond to the clusters. In addition, electron microscopy of freeze-fracture replicas shows regions that correspond to the clusters (Larabell and Chandler, 1988).

The ER clusters are not present in immature oocytes. Small clusters first appear in the vegetal cortex at about the time of nuclear envelope breakdown and disappear after ~1 h, and then large clusters appear at about the time the second meiotic metaphase block is reached. The annulate lamellae in the immature oocyte disappeared by the time of GVBD; this is expected because the annulate lamellae have many properties similar to the nuclear envelope (Kessel, 1992). These observations suggest that changes in the organization of ER are coupled with the cell cycle, very likely through maturation promoting factor activity.

Frog eggs are activated by IP_3-mediated Ca^{2+} release from the ER at fertilization (Han and Nuccitelli, 1990; Nuccitelli *et al.*, 1993; Stith *et al.*, 1993; Snow *et al.*, 1996; Runft *et al.*, 1999). The ER clusters in mature eggs contain IP_3 receptors, as shown by immunofluorescence, so that the clusters very probably release Ca^{2+} at fertilization. The appearance of the clusters correlates well with the timing of maturation, i.e.,
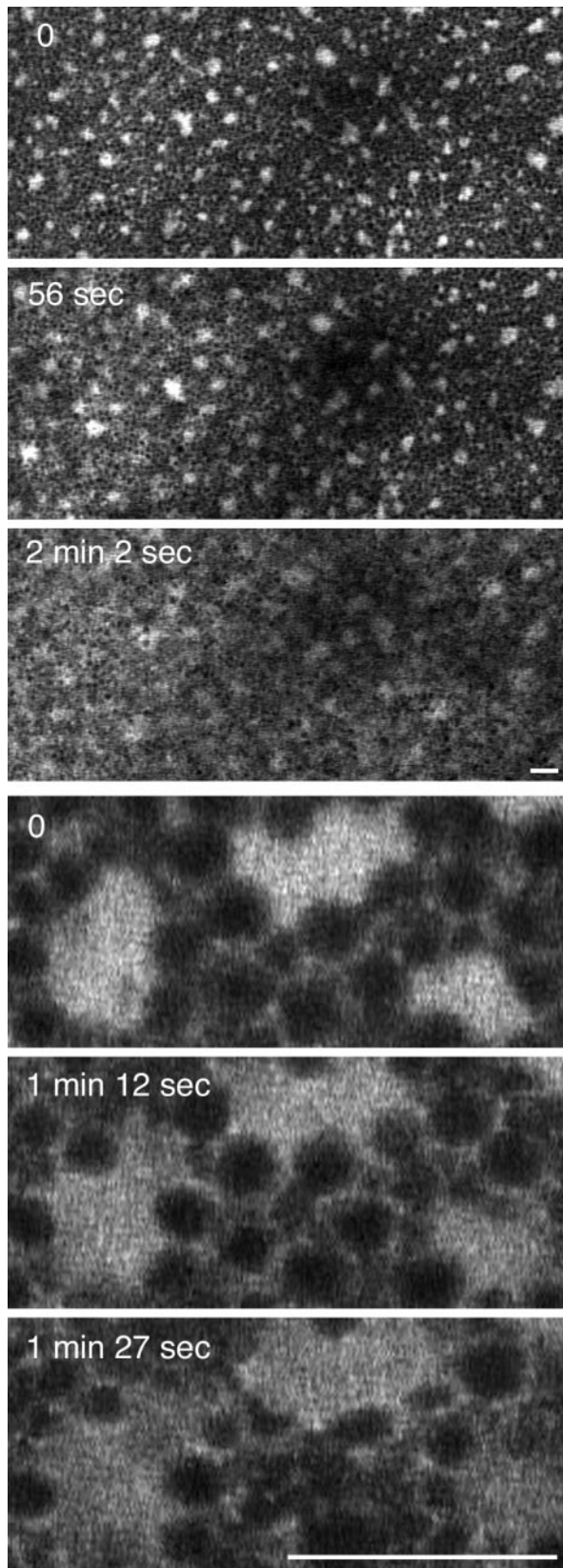
when the eggs become fertilizable. We show also that, as in starfish (Chiba *et al.*, 1990), hamster (Fujiwara *et al.*, 1993), and mouse (Mehlmann and Kline, 1994), maturation corresponds to increased sensitivity of Ca^{2+} release in response to IP_3. It therefore seems likely that the change in organization of the vegetal half ER is related in some way to the changes in calcium regulation that occur during maturation (see further discussion below).

When eggs were artificially activated, the ER clusters became dispersed. Because of the relative difficulty of fertilizing in vitro matured eggs, we did not test whether ER clusters dispersed during fertilization. There is no convenient calcium indicator dye that could be used for double labeling with GFP–KDEL, so we resorted to indirect means to see how the structural change was related temporally to Ca^{2+} release from the ER. We made use of a method developed in sea urchin eggs for imaging exocytosis with extracellular fluorescent dextran (Terasaki, 1995). The extracellular dextran patterns were found to lag 5–7 s behind the Ca^{2+} wave; this is very similar to sea urchins, where a similar lag occurs (Terasaki, 1995). Although we did not demonstrate in frog that extracellular dextran labeling corresponds to exocytosis, it seems that the Ca^{2+} increase at fertilization takes a relatively long time to trigger exocytosis. In double-labeling experiments, the extracellular dextran was imaged simultaneously with the ER changes. It appears that the dispersal begins simultaneous with, or after, the ER releases Ca^{2+}.

As noted previously (Kline *et al.*, 1999), the ER change in frog eggs fits a pattern among the eggs of species that have been investigated so far. The ER structure changes at fertilization in sea urchin (Terasaki and Jaffe, 1991; Jaffe and Terasaki, 1993), starfish (Jaffe and Terasaki, 1994; Terasaki *et al.*, 1996), and now *Xenopus* eggs, all of which have a single Ca^{2+} transient at fertilization, whereas the ER structure does not appear to change at fertilization in ascidian (Speksnijder *et al.*, 1993), *C. lacteus* (Stricker *et al.*, 1998), and mouse eggs (Kline *et al.*, 1999), all of which have multiple Ca^{2+} transients. It was proposed that the change in ER at fertilization somehow prevents the multiple Ca^{2+} waves (Kline *et al.*, 1999). One possibility is that movement of counter ions is involved. When Ca^{2+} is released from the ER, K^+ ions are likely to move into the ER to neutralize the loss of Ca^{2+} divalent cations (Meissner, 1983); however, the movement of two monovalent ions is required to electrically neutralize one Ca^{2+} ion, which should lead to osmotic imbalance. Presumably, the ER normally has mechanisms to compensate for this, but if these mechanisms are blocked or modified, Ca^{2+} release could cause such a large water influx resulting from osmotic imbalance that the ER continuity becomes disrupted or altered in morphology, preventing further Ca^{2+} release.

Figure 9. Dispersal of GFP–KDEL-labeled ER clusters in the vegetal cortex during artificial activation. The egg was prick activated with a micro-needle, and then the egg was repositioned so that the vegetal cortex could be observed. The Ca^{2+} wave that is initiated by the prick activation takes 1–2 min to reach the region that is imaged. These two image sequences show the change in ER structure that occurs. The top three panels are a low-magnification sequence, and the bottom three panels show a higher-magnification view. Bars, 10 μm.
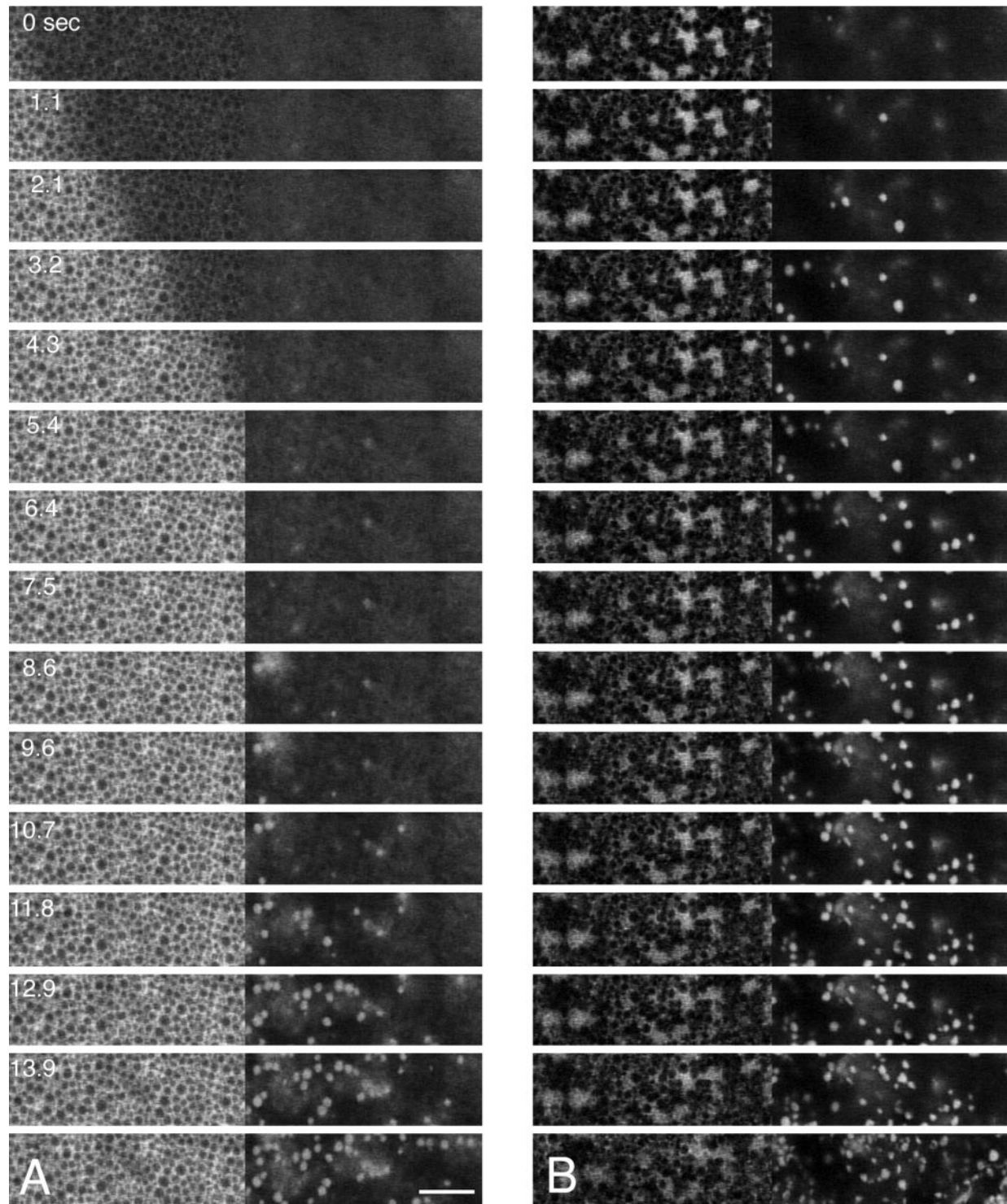
Figure 10. Relationship of the ER change at activation to surface changes. (A) Double labeling with intracellular Ca green dextran (left panels) and extracellular 3-kDa rhodamine dextran (right panels). In sea urchin eggs, extracellular dextrans label exocytotic pits that result from fusion of the cortical granules (Terasaki, 1995); it appears that extracellular dextran labels frog eggs similarly. Time interval between frames is 1.07 s. The increase in Ca^{2+} precedes the first appearance of extracellular dextran-labeled spots by 5–7 s. (B) Double labeling with GFP–KDEL (left panels) and extracellular rhodamine dextran (right panels). Changes in the ER seem to start to occur after or at the same time as the first appearance of extracellular dextran-labeled spots. Because the Ca^{2+} rise precedes the extracellular dextran-labeled spots, this indicates that the changes in the ER begin to occur ~5–7 s after the release of Ca^{2+}. Bar, 10 μm.

The ER clusters that develop during maturation in *Xenopus* oocytes closely resemble the clusters of ER that appear during maturation in mouse (Mehlmann *et al.*, 1995), hamster (Shiraishi *et al.*, 1995), and *C. lacteus* (Stricker *et al.*, 1998) oocytes. In mouse, the clusters were shown to contain the type I IP$_3$ receptor (Mehlmann *et al.*, 1996); their size is comparable to those of frog, and thin-section electron micrographs show a similar ultrastructure (Hand, Mehlmann, and Terasaki, unpublished results). It is curious that the clusters are found on the side opposing the meiotic spindle in all of these species. Fertilization in mouse occurs on this side, whereas fertilization in frog occurs on the animal or opposite side, so that the clusters apparently are not related to the initial release of Ca^{2+} at fertilization. In mouse (Kline *et al.*, 1999; Deguchi *et al.*, 2000) and *C. lacteus* (Stricker *et al.*, 1998), it seems likely that the clusters are involved in the initiation of the secondary Ca^{2+} waves because these originate from the side containing the clusters.

One possibility is that the ER clusters serve to concentrate Ca^{2+} release channels in a small region of cytoplasm. Localization of voltage-gated sodium channels in the plasma membrane of neurons has distinct functional consequences (Kandel *et al.*, 2000). Sodium channels are highly concentrated at the initial segment of neurons. If the membrane potential at this location is depolarized past a threshold by synaptic depolarizations, the sodium channels initiate an action potential. In many large-diameter axons, sodium channels are also present at high concentrations at the nodes of Ranvier. These sodium channels are involved in saltatory propagation of the action potential, with a resulting faster rate and more efficient transmission. In a similar way, the ER clusters could serve to concentrate IP$_3$ receptors to help in initiating and/or propagating Ca^{2+} signals. In eggs with multiple Ca^{2+} transients, the clusters of ER could act as an initiating region for the secondary Ca^{2+} waves. In frog eggs, the clusters may help propagate the Ca^{2+} wave in the vegetal half.

One reason why it may be necessary to facilitate Ca^{2+} wave propagation in the vegetal half of the frog egg is related to the abundance of yolk. The yolk platelets are large organelles that collectively occupy at least half of the cytoplasmic volume. They are distributed throughout the interior up to ~5 μm of the surface, and they are significantly larger and more abundant in the vegetal half (Danilchik and Gerhart, 1987). By occupying space, they can hinder propagation of Ca waves by reducing the density of IP$_3$ receptors (because of the lower amount of space available for the ER) and by restricting the possible diffusion paths for Ca^{2+} to spread. ER clusters containing many IP$_3$ receptors may serve to counteract these effects of reduced space. We plan to use computer modeling (Fink *et al.*, 1999) to investigate whether the clusters help ensure propagation in this way.

It has generally been difficult to understand how structure and function of the ER are related. Part of the problem is basic uncertainties about the "geometry" and dynamics of the ER. In the thinly spread periphery of fibroblasts, the ER is a network of tubules connected by three-way junctions, and tubules are extended through an interaction with microtubules (Terasaki *et al.*, 1986; Waterman-Storer and Salmon, 1998); however, the ER in thicker regions of cells is much less well understood. It has been shown that network formation from disrupted ER in *Xenopus* extracts is indepen-

dent of the cytoskeleton (Dreier and Rapoport, 2000). Little is known about why the ER membranes take the form of tubules or cisternae, and it is not known how these elements are connected in a three-dimensional structure. One interesting possibility is that cisternae form mobius strip-related structures. In such structures, a molecule could diffuse throughout the membrane without having to pass an area of high curvature, and such structures cannot close in on themselves to isolate regions of cytoplasm. An important property of the ER that is closely related to these structural issues is compartmentalization; there is little knowledge of how molecules and functions are compartmentalized in the ER. The use of GFP chimeras in living cells should aid in investigating this in the near future. The ER can have complex properties through its distribution and compartmentalization, and it seems certain that knowledge of ER organization is important for understanding cell function.

ACKNOWLEDGMENTS

REFERENCES

Campanella, C., and Andreuccetti, P. (1977). Ultrastructural observations on cortical endoplasmic reticulum and on residual cortical granules in the egg of *Xenopus laevis*. Dev. Biol. *56*, 1–10.

Campanella, C., Andreuccetti, P., Taddei, C., and Talevi, R. (1984). The modifications of cortical endoplasmic reticulum during in vitro maturation of *Xenopus laevis* oocytes and its involvement in cortical granule exocytosis. J. Exp. Zool. *229*, 283–293.

Carroll, D.J., Albay, D.T., Terasaki, M., Jaffe, L.A., and Foltz, K.R. (1999). Identification of PLCgamma-dependent and -independent events during fertilization of sea urchin eggs. Dev. Biol. *206*, 232–247.

Carroll, D.J., Ramarao, C.S., Mehlmann, L.M., Roche, S., Terasaki, M., and Jaffe, L.A. (1997). Calcium release at fertilization is mediated by phospholipase Cγ. J. Cell Biol. *138*, 1303–1311.

Carroll, J. (2000). Na$^+$ – Ca^{2+} exchange in mouse oocytes: modifications in the regulation of intracellular free Ca^{2+} during oocyte maturation. J. Reprod. Fertil. *118*, 337–342.

Chandler, D.E., and Heuser, J.E. (1979). Membrane fusion during secretion. Cortical granule exocytosis in sea urchins studied by quick-freezing and freeze fracture. J. Cell Biol. *83*, 91–108.

Charbonneau, M., and Gray, R.D. (1984). The onset of activation responsiveness during maturation coincides with the formation of the cortical endoplasmic reticulum in oocytes of *Xenopus laevis*. Dev. Biol. *102*, 90–97.

Chiba, K., Kado, R.T., and Jaffe, L.A. (1990). Development of calcium release mechanisms during starfish oocyte maturation. Dev. Biol. *140*, 300–306.

Danilchik, M.V., and Gerhart, J.C. (1987). Differentiation of the animal-vegetal axis in *Xenopus laevis* oocytes. I. Polarized intracellular translocation of platelets establishes the yolk gradient. Dev. Biol. *122*, 101–112.

Deguchi, R., Shirakawa, H., Oda, S., Mohri, T., and Miyazaki, S. (2000). Spatiotemporal analysis of Ca^{2+} waves in relation to the

sperm entry site and animal-vegetal axis during Ca^{2+} oscillations in fertilized mouse eggs. Dev. Biol. *218*, 299–313.

Dreier, L., and Rapoport, T.A. (2000). In vitro formation of the endoplasmic reticulum occurs independently of microtubules by a controlled fusion reaction. J. Cell Biol. *148*, 883–898.

Duesbery, N.S., and Masui, Y. (1993). Changes in protein association with intracellular membranes of *Xenopus laevis* oocytes during maturation and activation. Zygote *1*, 129–141.

Eisen, A., and Reynolds, G.A. (1985). Sources and sinks for the calcium released during fertilization of single sea urchin eggs. J. Cell Biol. *100*, 1522–1527.

Fink, C.C., Slepchenko, B., Moraru, I.I., Schaff, J., Watras, J., and Loew, L.M. (1999). Morphological control of inositol-1,4,5-trisphosphate-dependent signals. J. Cell Biol. *147*, 929–936.

Fujiwara, T., Nakada, K., Shirakawa, H., and Miyazaki, S. (1993). Development of inositol trisphosphate-induced calcium release mechanism during maturation of hamster oocytes. Dev. Biol. *156*, 69–79.

Gallo, C.J., Hand, A.R., Jones, T.L.Z., and Jaffe, L.A. (1995). Stimulation of *Xenopus* oocyte maturation by inhibition of the G-protein αs subunit, a component of the plasma membrane and yolk platelet membranes. J. Cell Biol. *130*, 275–284.

Gard, D.L. (1992). Microtubule organization during maturation of *Xenopus* oocytes: assembly and rotation of the meiotic spindles. Dev. Biol. *151*, 516–530.

Gardiner, D.M., and Gray, R.D. (1983). Membrane junctions in *Xenopus* eggs: their distribution suggests a role in calcium regulation. J. Cell Biol. *96*, 1159–1163.

Han, J.K., and Nuccitelli, R. (1990). Inositol 1,4,5-trisphosphate-induced calcium increase in the organelle layers of the stratified, intact egg of *Xenopus laevis*. J. Cell Biol. *110*, 1103–1110.

Henson, J.H., Beaulieu, S.M., Kaminer, B., and Begg, D.A. (1990). Differentiation of a calsequestrin-containing endoplasmic reticulum during sea urchin oogenesis. Dev. Biol. *142*, 255–269.

Imoh, H., Okamoto, M., and Eguchi, G. (1983). Accumulation of annulate lamellae in the subcortical layer during progesterone-induced oocyte maturation in *Xenopus laevis*. Dev. Growth Differ. *25*, 1–10.

Jaffe, L.A., Giusti, A.F., Carroll, D.J., and Foltz, K.R. (2001). Ca^{2+} signaling during fertilization of echinoderm eggs. Sem. Cell Dev. Biol. *12*, 45–51.

Jaffe, L.A., and Terasaki, M. (1993). Structural changes of the endoplasmic reticulum of sea urchin eggs during fertilization. Dev. Biol. *156*, 556–573.

Jaffe, L.A., and Terasaki, M. (1994). Structural changes in the endoplasmic reticulum of starfish oocytes during meiotic maturation and fertilization. Dev. Biol. *164*, 579–587.

Kandel, E.R., Schwartz, J.H., and Jessell, T.M. (2000). Principles of Neural Science, 4th ed., New York: McGraw-Hill Co.

Kessel, R.G. (1992). Annulate lamellae: a last frontier in cellular organelles. Int. Rev. Cytol. *133*, 43–120.

Kline, D. (1988). Calcium-dependent events at fertilization of the frog egg: injection of a calcium buffer blocks ion channel opening, exocytosis, and formation of pronuclei. Dev. Biol. *126*, 346–361.

Kline, D., Mehlmann, L., Fox, C., and Terasaki, M. (1999). The cortical ER of the mouse egg: localization of ER clusters in relation to the generation of repetitive calcium waves. Dev. Biol. *215*, 431–442.

Kume, S., Muto, A., Aruga, J., Nakagawa, T., Michikawa, T., Furuichi, T., Nakade, S., Okano, H., and Mikoshiba, K. (1993). The *Xeno-*

pus IP_3 receptor: structure function and localization in oocytes and eggs. Cell *73*, 555–570.

Kume, S., Yamamoto, A., Inoue, T., Muto, A., Okano, H., and Mikoshiba, K. (1997). Developmental expression of the inositol 1,4,5-trisphosphate receptor and structural changes in the endoplasmic reticulum during oogenesis and meiotic maturation of *Xenopus laevis*. Dev. Biol. *182*, 228–239.

Larabell, C.A., and Chandler, D.E. (1988). Freeze-fracture analysis of structural reorganization during meiotic maturation in oocytes of *Xenopus laevis*. Cell. Tissue Res. *251*, 129–136.

Lucero, H.A., Lebeche, D., and Kaminer, B. (1994). ER calcistorin/ protein disulfide isomerase (PDI): sequence determination and expression of a cDNA clone encoding a calcium storage protein with PDI activity from endoplasmic reticulum of the sea urchin egg. J. Biol. Chem. *269*, 23112–23119.

Masui, Y., and Clarke, H.J. (1979). Oocyte maturation. Int. Rev. Cytol. *57*, 185–282.

Mehlmann, L.M., and Kline, D. (1994). Regulation of intracellular calcium in the mouse egg: calcium release in response to sperm or inositol trisphosphate is enhanced after meiotic maturation. Biol. Reprod. *51*, 1088–1098.

Mehlmann, L.M., Mikoshiba, K., and Kline, D. (1996). Redistribution and increase in cortical inositol 1,4,5-trisphosphate receptors after meiotic maturation of the mouse oocyte. Dev. Biol. *180*, 489–498.

Mehlmann, L.M., Terasaki, M., Jaffe, L.A., and Kline, D. (1995). Reorganization of the endoplasmic reticulum during meiotic maturation of the mouse oocyte. Dev. Biol. *170*, 607–615.

Meissner, G. (1983). Monovalent ion and calcium ion fluxes in sarcoplasmic reticulum. Mol. Cell. Biochem. *55*, 65–82.

Miyazaki, S., Shirakawa, H., Nakada, K., and Honda, Y. (1993). Essential role of the inositol 1,4,5-trisphosphate receptor/Ca^{2+} release channel in Ca^{2+} waves and Ca^{2+} oscillations at fertilization of mammalian eggs. Dev. Biol. *148*, 62–78.

Miyazaki, S., Yuzaki, M., Nakada, K., Shirakawa, H., Nakanishi, S., Nakade, S., and Mikoshiba, K. (1992). Block of Ca^{2+} wave and Ca^{2+} oscillation by antibody to the inositol 1,4,5-trisphosphate receptor in fertilized hamster eggs. Science *257*, 251–255.

Nuccitelli, R., Yim, D.L., and Smart, T. (1993). The sperm-induced Ca^{2+} wave following fertilization of the *Xenopus* egg requires the production of $Ins(1,4,5)P_3$. Dev. Biol. *158*, 200–212.

Parys, J.B., McPherson, S.M., Mathews, L., Campbell, K.P., and Longo, F.J. (1994). Presence of inositol 1,4,5-trisphosphate receptor, calreticulin, and calsequestrin in eggs of sea urchins and *Xenopus laevis*. Dev. Biol. *161*, 466–476.

Runft, L.L., Watras, J., and Jaffe, L.A. (1999). Calcium release at fertilization of *Xenopus* eggs requires type I IP3 receptors, but not SH2 domain-mediated activation of PLC-γ or G_q-mediated activation of PLCβ. Dev. Biol. *214*, 399–411.

Shearer, J., De Nadai, C., Emily-Fenouil, F., Gache, C., Whitaker, M., and Ciapa, B. (1999). Role of phospholipase C gamma at fertilization and during mitosis in sea urchin eggs and embryos. Development *126*, 2273–2284.

Shiraishi, K., Okada, A., Shirakawa, H., Nakanishi, S., Mikoshiba, K., and Miyazaki, S. (1995). Developmental changes in the distribution of the endoplasmic reticulum and inositol 1,4,5-trisphosphate receptors and the spatial pattern of Ca^{2+} release during maturation of hamster oocytes. Dev. Biol. *170*, 594–606.

Snow, P., Yim, D.L., Leibow, J.D., Saini, S., and Nuccitelli, R. (1996). Fertilization stimulates an increase in inositol trisphosphate and inositol lipid levels in *Xenopus* eggs. Dev. Biol. *180*, 108–118.

Speksnijder, J.E., Terasaki, M., Hage, W.J., Jaffe, L.F., and Sardet, C. (1993). Polarity and reorganization of the endoplasmic reticulum

during fertilization and ooplasmic segregation in the ascidian egg. J. Cell. Biol. *120*, 1337–1346.

Stith, B.J., Goalstone, M., Silva, S., and Jaynes, C. (1993). Inositol 1,4,5-trisphosphate mass changes from fertilization through first cleavage in *Xenopus laevis*. Mol. Biol. Cell *4*, 435–443.

Stricker, S.A. (1999). Comparative biology of calcium signaling during fertilization and egg activation in animals. Dev. Biol. *211*, 157–176.

Stricker, S.A., Centonze, V.E., and Melendez, R.F. (1994). Calcium dynamics during starfish oocyte maturation and fertilization. Dev. Biol. *166*, 34–58.

Stricker, S.A., Silva, R., and Smythe, T. (1998). Calcium and endoplasmic reticulum dynamics during oocyte maturation and fertilization in the marine worm *Cerebratulus lacteus*. Dev. Biol. *203*, 305–322.

Terasaki, M. (1995). Visualization of exocytosis during sea urchin egg fertilization using confocal microscopy. J. Cell Sci. *108*, 2293–2300.

Terasaki, M. (2000). Dynamics of the ER and Golgi apparatus during early sea urchin development. Mol. Biol. Cell *11*, 897–914.

Terasaki, M., Chen, L.B., and Fujiwara, K. (1986). Microtubules and the endoplasmic reticulum are highly interdependent structures. J. Cell Biol. *103*, 1557–1568.

Terasaki, M., and Jaffe, L.A. (1991). Organization of the sea urchin egg endoplasmic reticulum and its reorganization at fertilization. J. Cell Biol. *114*, 929–940.

Terasaki, M., Jaffe, L.A., Hunnicutt, G.R., and Hammer, J.A., III (1996). Structural change of the endoplasmic reticulum during fertilization: evidence for loss of membrane continuity using the green fluorescent protein. Dev. Biol. *179*, 320–328.

Waterman-Storer, C.M., and Salmon, E.D. (1998). Endoplasmic reticulum membrane tubules are distributed by microtubules in living cells using three distinct mechanisms. Curr. Biol. *8*, 798–806.

Whalley, T., Terasaki, M., Cho, M.-S., and Vogel, S.S. (1995). Rapid membrane retrieval following exocytosis in sea urchin eggs. J. Cell Biol. *131*, 1183–1192.

Yumura, S., and Fukui, Y. (1985). Reversible cyclic AMP-dependent change in distribution of myosin thick filaments in *Dictyostelium*. Nature *314*, 194–196.